ChemPubSoc Europe

DOI: 10.1002/open.201800059

Open Access ChemistryOPEN Full Papers

Partial Substitution of Potassium with Sodium in the $K_2Ti_2(PO_4)_3$ Langbeinite-Type Framework: Synthesis and Crystalline Structure of $K_{1.75}Na_{0.25}Ti_2(PO_4)_3$

Igor V. Zatovsky,[a] Nataliia Yu. Strutynska,[b] Yuriy A. Hizhnyi,[b] Sergiy G. Nedilko,[b] Nickolai S. Slobodyanik,[b] and Nickolai. I. Klyui*[a, c]

The interaction of TiN with Na_2O–K_2O–P_2O_5 melts was investigated at (Na + K)/P molar ratios of 0.9, 1.0, and 1.2 and at Na/K molar ratios of 1.0 and 2.0. Interactions in the system led to the loss of nitrogen and the partial loss of phosphorus and resulted in the formation of $KTiP_2O_7$ and langbeinite-type $K_{2-x}Na_xTi_2(PO_4)_3$ ($x = 0.22$–0.26) solid solutions over the temperature range of 1173 to 1053 K. The phase compositions of the obtained samples were determined by using X-ray diffraction (including Rietveld refinement), scanning electron microscopy (using energy-dispersive X-ray spectroscopy and element mapping), FTIR spectroscopy, and thermogravimetric analysis/differential thermal analysis. $K_{1.75}Na_{0.25}Ti_2(PO_4)_3$ was characterized by single-crystal X-ray diffraction [$P2_13$ space group, $a = 9.851(5)$ Å]. The 3D framework is built up by TiO_6 octahedra and PO_4 tetrahedra sharing all the oxygen vertices with the formation of cavities occupied by K(Na) cations. Only one of the two crystallographically inequivalent potassium sites is partially substituted by sodium, and this was confirmed by calculating the bond-valence sum. The thermodynamic stability of $K_{1.75}Na_{0.25}Ti_2(PO_4)_3$ crystals and the preferable occupation sites of Na_K cationic substitutions were investigated by DFT-based electronic structure calculations performed by the plane-wave pseudopotential method.

1. Introduction

Transition-metal complex phosphates have found widespread practical applications as electrode materials in Li-ion batteries (LIBs).[1,2] Currently, this family of compounds is under extensive investigation to create next-generation cathode materials for sodium-ion batteries (NIBs)[2–5] and asymmetric solid-state supercapacitors.[6] Sodium-ion batteries (NIBs) generally exhibit lower theoretical capacity and cell potential than LIBs. At the same time, sodium is cheaper, nontoxic, and more abundant than lithium. As a result, NIBs have recently attracted increasing research interest. In particular, a number of open 3D-framework phosphates of NASICON (NAtrium Super Ionic CONductor)[2,4,5] and olivine-type[3–5] structures, several fluorophosphates,[5,7] and layered 2D-framework phosphates [e.g. $M^I_4M^{II}_3(PO_4)_2P_2O_7$ mixed-anionic compounds][8,9] were proposed as bases for cathode or anode materials with stable cyclic characteristics. Among these materials, the best battery performance was observed for NASICON-type structures due to their high sodium conductivity and good stability in redox reactions.[2] The composition of polyanionic compounds with the langbeinite-type structure is very similar to the composition of NASICON-type ones, and this is why langbeinite-type compounds are also considered possible new hosts for electrode materials.[10]

The general composition of compounds comprising phosphates of alkali and multivalent metals with NASICON-type structures can be characterized by the following formula: $M^I_xZ_2(PO_4)_3$ (M^I = Li, Na; Z = aliovalent metal or metals; $x = 1.0$–4.0). The structure is built up by a three-dimensional framework of ZO_6 octahedra and PO_4 tetrahedra sharing all the oxygen vertices; the $[Z_2(PO_4)_3]$ unit stands out as a constitutional block of the framework. Within the framework, the alkali metal may occupy two sites: M1 (special position) or M2 (general position that can remain partially or completely vacant). The general composition of $M^I_xZ_2(PO_4)_3$ includes two types of $[Z_2(PO_4)_3]$ unit packaging, which depends on the aggregation of the framework blocks in the three-dimensional structure. The first variant belongs to the $Sc_2(WO_4)_3$ structural type (SW-type).[11] Here, the crystalline lattice may include only cations with small ionic radii (lithium), for example, α-$Li_3V_2(PO_4)_3$ phosphate.[12] The second packaging, associated with the formation

[a] Prof. I. V. Zatovsky, Prof. N. I. Klyui
College of Physics, Jilin University
2699 Qianjin St., 130012 Changchun (P. R. China)
E-mail: klyuini@ukr.net

[b] Dr. N. Y. Strutynska, Dr. Y. A. Hizhnyi, Prof. S. G. Nedilko, Prof. N. S. Slobodyanik
Taras Shevchenko National University
64/13 Volodymyrska Str., 01601 Kyiv (Ukraine)

[c] Prof. N. I. Klyui
Lashkaryov Institute of Semiconductor Physics
NAS of (UK)raine, 41 Pr. Nauki, 03028 Kyiv (Ukraine)

Supporting Information and the ORCID identification number(s) for the author(s) of this article can be found under: https://doi.org/10.1002/open.201800059.

of the langbeinite-type structure $[K_2Mg_2(SO_4)_3]$,[13] determines the presence of big cations in the framework. This results in the general chemical formula $M^I_xZ_2(PO_4)_3$ (M^I = K, Rb, Cs; Z = aliovalent metal or metals; $1.0 \le x \le 2.0$) for stoichiometric compounds or solid solutions, for example, $K_{2-x}Ti_2(PO_4)_3$,[14,15] $K_2M^{III}Ti(PO_4)_3$ (M^{III} = Al,[16] Er, Yb, or Y),[17] $K_2M^{II}_{0.5}Ti_{1.5}(PO_4)_3$ (M^{II} = Ni,[18] Co, or Mn),[19] $Rb_2Yb_xTi_{2-x}(PO_4)_3$,[20,21] and $Cs_{1+x}Ln_xZr_{2-x}(PO_4)_3$ (Ln = Sm–Lu).[22]

Due to their high thermal and chemical stability, langbeinite-type phosphates are intensively studied as matrixes for the storage of radioactive waste from the nuclear industry[23] and as basic materials for luminophores.[24] However, if the lattice is formed from big alkaline cations (e.g. K, Rb, Cs), effective ionic conductivity is achieved only at elevated temperatures. Notably, a few Na-containing langbeinite-type complex phosphates have been obtained, and the existing examples are limited to $Na_2M^{III}Ti(PO_4)_3$ (M^{III} = Cr, Fe).[25] At present, much research effort is being directed to the synthesis of novel battery materials that simultaneously possess the langbeinite-type structure and light cations.[10] These efforts are based on the following two-stage approach: 1) to design host structures by using a specific type of cation (e.g. K^+); 2) to extract these specific ions (by ionic substitution or chemical oxidation) to obtain a framework for reversible de/intercalation of Na^+ (or Li^+). However, the application of this approach is not successful for the extraction of K^+ from langbeinite-type frameworks, as illustrated by attempts with $K_2Fe_2(SO_4)_2$[10] and $K_2TiV(PO_4)_3$.[26]

Another way to search for novel langbeinite-type phosphates with sufficient ionic conductivity is to obtain compounds containing both big K^+ cations and small Na^+ cations. Recently, the synthesis of a langbeinite-type solid solution with the chemical formula $K_{0.877}Na_{0.48}Ti_2(PO_4)_3$ was reported.[27] Reliable information about the structure, stability, and formation principles is crucially important for further study of such kinds of materials. Motivated by this need, we directed our efforts to the synthesis of K–Na-containing complex phosphates of the langbeinite type to obtain single crystals for X-ray diffraction analysis to enable structural analysis and further theoretical calculation of the electronic structure and related properties.

For this purpose, the features of the interactions of TiN with the Na_2O–P_2O_5 and K_2O–P_2O_5 melts[15] were analyzed, and the possibility to form $K_{2-x}Na_xTi_2(PO_4)_3$ solid solutions was predicted for the case of combined K–Na-containing phosphate melts. This possibility was successfully realized, and the corresponding synthesis procedures are described in the present paper. Here, in particular, the special aspects of the interaction of TiN with K_2O–Na_2O–P_2O_5 melts are analyzed, and conditions for the formation of complex titanium phosphates [including langbeinite-related solid solutions $K_{2-x}Na_xTi_2(PO_4)_3$, denoted here as L-KNTP] are determined. The obtained samples were characterized by X-ray diffraction (XRD), scanning electron microscopy (SEM), FTIR spectroscopy, and thermogravimetric and differential thermal analysis (TG/DTA) techniques.

According to the XRD and SEM results [using energy-dispersive X-ray spectroscopy (EDS) analysis and element mapping], the composition of the L-KNTP crystal is close to $K_{1.75}Na_{0.25}Ti_2(PO_4)_3$. The X-ray results also indicate that only one of the two crystallographically inequivalent potassium sites in the L-KNTP structure are partially substituted by sodium. The thermodynamic stability of $K_{1.75}Na_{0.25}Ti_2(PO_4)_3$ crystals and the preferential occupation of the alkaline metals sites at cationic substitutions ($K^+ \rightarrow Na^+$) were investigated by DFT-based electronic structure calculations performed by the plane-wave pseudopotential method. The calculations confirmed the stability of the $K_{1.75}Na_{0.25}Ti_2(PO_4)_3$ structure.

2. Results and Discussion

2.1. Interaction of TiN with Molten Na_2O–K_2O–P_2O_5

Analysis of previously reported results for the interaction of TiO_2 with mixed phosphate melts such as Na_2O–K_2O–P_2O_5 showed that the formation of langbeinite-related phosphate took place at molar ratios of (Na + K)/P = 0.9 and Na/K = 1.0.[27] Structure determination of $K_{0.877}Na_{0.48}Ti^{III}_{0.357}Ti^{IV}_{1.643}(PO_4)_3$ showed partial substitution of K^+ by Na^+ and the formation of vacancies in the crystallographic positions of the alkaline metals.[27] This latter fact significantly complicates estimation of the possibility to substitute potassium by sodium in the langbeinite-related structure. At the same time, interaction of TiN with the M^IO_2-P_2O_5 melt (M^I = alkaline metal) is a convenient way to obtain mixed-valent complex phosphates with a Ti^{III}/Ti^{IV} ratio of 1.0.[15] Moreover, this technique allows the growth of crystals that are sufficiently large for X-ray diffraction studies. For this reason, this approach was chosen to obtain crystals of solid solutions of L-KNTP.

On the basis of previous results,[15,27] the interactions of TiN with Na_2O–K_2O–P_2O_5 melts were studied in this work at (Na + K)/P molar ratios ranging from 0.9 to 1.2 to identify a route to fabricate L-KNTP solid solutions. To achieve competitive conditions for sodium and potassium in the self-flux, two values of the initial Na/K ratio (1.0 and 2.0) and a fixed value of added TiN (3.0 wt%) were selected. As shown in Ref. [15], such a quantity of TiN allows complex phosphates to be obtained and prevents significant changes in the phosphorus content in the self-flux.

At Na/K = 2.0, the rate of TiN dissolution in mixed Na–K phosphate fluxes was significantly higher than that in only sodium or potassium phosphate fluxes. Crystallization of the self-flux at Na/K = 2.0 and over the (Na + K)/P = 0.9–1.2 range did not result in the formation of crystals (melt transformed into glass).

The crystalline phases were obtained in all cases with equal contents of sodium and potassium in the initial melts (Na/K = 1.0). According to the XRD data, in the P_2O_5-rich melt [(Na + K)/P = 0.9] a mixture of $KTiP_2O_7$/TiN in a ratio of approximately 2:1 is obtained (Figure 1, curve 1). Optical microscopy analysis of these samples shows that the $KTiP_2O_7$ crystals contain dark inclusions of titanium nitride. Consequently, phosphate $KTiP_2O_7$ is poorly soluble in such a melt and its crystallization occurs on the surface of TiN that has not been pre-reacted. This process blocks further dissolution of TiN and leads to the generation of a diphase sample. The formation of $KTiP_2O_7$ is also supported by the FTIR spectroscopy results, as shown in Figure 2, curve 1

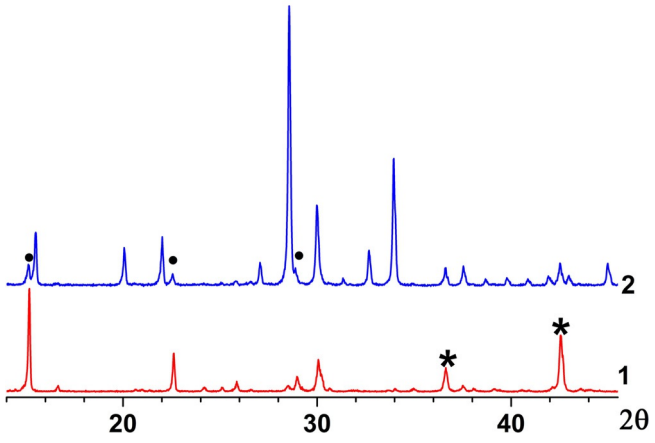

Figure 1. X-ray diffraction patterns of the obtained samples: curve 1) $KTiP_2O_7$ + TiN (* denotes TiN); curve 2) $K_{1.75}Na_{0.25}Ti_2(PO_4)_3$ + $KTiP_2O_7$ heated to 1173 K (● denotes $KTiP_2O_7$).

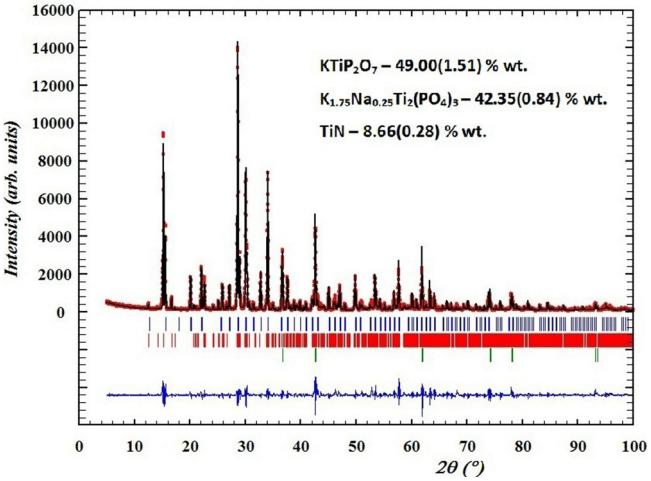

Figure 3. Rietveld refinement of the obtained $K_{1.75}Na_{0.25}Ti_2(PO_4)_3$ (blue vertical bars) + $KTiP_2O_7$ (red vertical bars) + TiN (green vertical bars) mixture. Experimental (dots), calculated (black curve), and difference (blue curve) data for $2\theta = 5–100°$.

(designation of the observed spectral signals is presented in Table S1 in the Supporting Information).

Increasing the (Na + K)/P ratio to 1.0 at Na/K = 1.0 in the initial melt led to an increase in its dissolving capability relative to that of TiN. Further cooling to 1053 K resulted in the formation of another type of dark-violet crystals. The appearance of the langbeinite-related phosphate crystals octahedral in form in the self-flux was observed at the first stage of cooling (1173–1123 K), which indicated their low solubility in the melt. According to Rietveld refinement (Figure 3), the obtained multiphase sample contains two types of phosphate crystals, namely, L-KNTP and $KTiP_2O_7$, in nearly equal proportions, and only 8.66(0.28) wt% of TiN, which did not pre-react. The infrared absorption spectrum of the obtained sample (Figure 2, curve 2) reveals the presence of absorption lines typical for both diphosphate and orthophosphate groups. This is additional evidence for the formation of a phosphate mixture (designation of the observed absorption bands for the langbeinite-type phase is presented in Table S1).

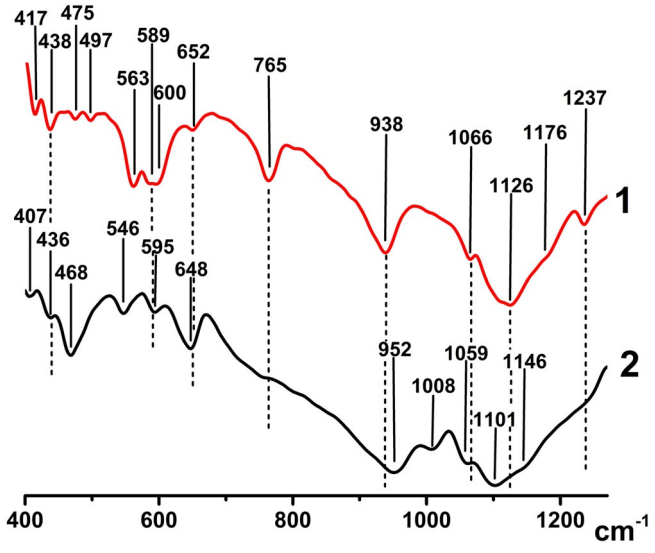

Figure 2. FTIR spectra of the obtained mixtures: curve 1) $KTiP_2O_7$ + TiN; curve 2) $K_{1.75}Na_{0.25}Ti_2(PO_4)_3$ + $KTiP_2O_7$.

The SEM images of the obtained samples reveal the presence of crystals of two different morphologies, and according to primary EDS analysis, a significant amount of sodium is found (Figure 4).

For $K_2Ti_2(PO_4)_3$ and $KTiP_2O_7$, the weight percentages of the elements are close (the difference does not exceed 3 wt%). Accordingly, with the aim to determine the degree of substitution of potassium by sodium in the two types of crystalline phases, EDS analysis and mapping of the elements for a number of separate crystals with different morphologies were conducted. An example of such a study is illustrated in Figure 5. As a rule, langbeinite-type crystals are octahedral faceting. In these crystals, the elements are evenly distributed (see Figure 5a), and the amount of sodium is in the range of 1.15 to 1.37 at% (these values were obtained by analyzing nine various spots of nine crystals of the L-KNTP-type; the spots are depicted by white rectangles in Figure 5). The obtained values correspond to compositions of solid solutions of $K_{2-x}Na_xTi_2(PO_4)_3$ with $x = 0.22–0.26$. This result is in good compliance with the X-ray data of a single crystal (see Section 2.3). For this reason, we can accept the $K_{1.75}Na_{0.25}Ti_2(PO_4)_3$ (L-KNTP) compound as the langbeinite-type phosphate. Crystallites of $KTiP_2O_7$ are formed as a three-dimensional distorted octahedron and grow preferentially in one direction (Figure 5b). EDS analysis of these crystals shows that the sodium content does not exceed 0.55 at%. This fact may be associated with the formation of $K_{1-x}Na_xTiP_2O_7$ ($x < 0.06$) solid solutions. At the same time, the map of the sodium element shows weak intensity and poor uniformity relative to the maps of the other elements (Figure 5b). Therefore, we think that the sodium in the crystals of $KTiP_2O_7$ is only a doping impurity.

An increase in the (Na + K)/P ratio to 1.2 in the initial melt leads to rapid TiN dissolution followed by oxidation of trivalent titanium. Cooling of such a self-flux causes the growth of only

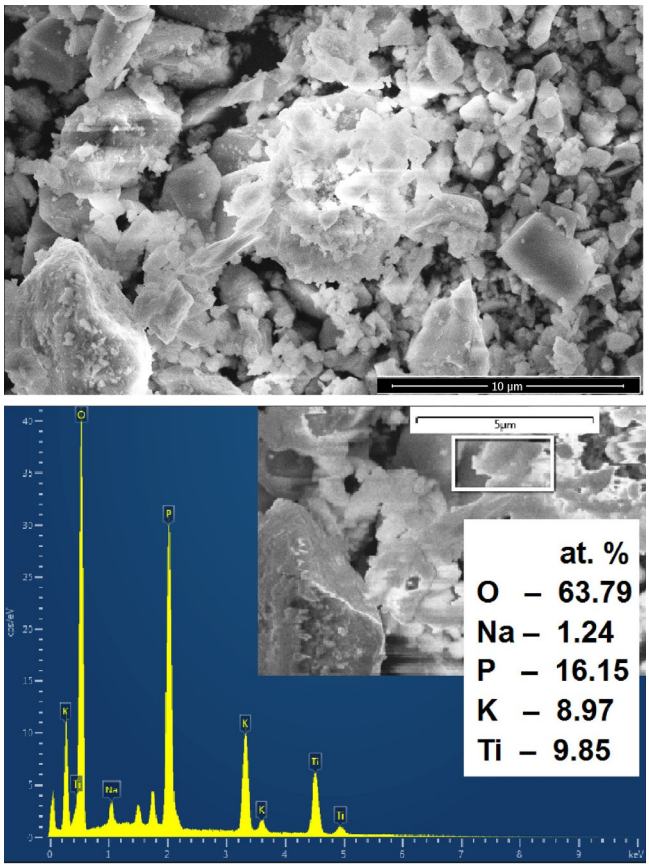

Figure 4. SEM images and EDS analysis of the obtained $K_{1.75}Na_{0.25}Ti_2(PO_4)_3 + KTiP_2O_7$ mixture.

a small amount of colorless and violet crystals. The FTIR spectra were recorded for two mechanically selected types of the obtained crystals (Figure S1). On the basis of the obtained FTIR spectroscopy results, the colorless crystals can be identified as the double phosphate, $NaTi_2(PO_4)_3$,[28] whereas violet crystals are langbeinite-related phosphate L-KNTP (micrographs of the samples are shown in Figure S2).

2.2. Study of Thermal Stability

The thermal stability of the obtained L-KNTP + $KTiP_2O_7$ sample was studied by thermogravimetric and differential thermal analysis (Figure S3). Three primary intervals can be marked out in the TG curve. The first is due to the loss of adsorbed water (≈1 wt%), which is finished completely before the temperature reaches 720 K. The other two intervals of 823–1073 and 1297–1410 K demonstrate sample weight gains of approximately 1.2 and 0.6 wt%, respectively. These processes are attributed to the oxidation of trivalent titanium to titanium(IV) by atmospheric oxygen, which should result in degradation of the obtained compounds. As both oxidation intervals are rather wide, such processes are not reflected in the DTA curve. At the same time, the DTA curve reveals a relatively wide peak corresponding to an endo effect with a maximum at 1408 K. This effect is caused by melting of the sample after oxidation of the entire amount of Ti^{III}. This scheme is supported by the formation of a colorless solidified melt after differential thermal analysis (Figure S4).

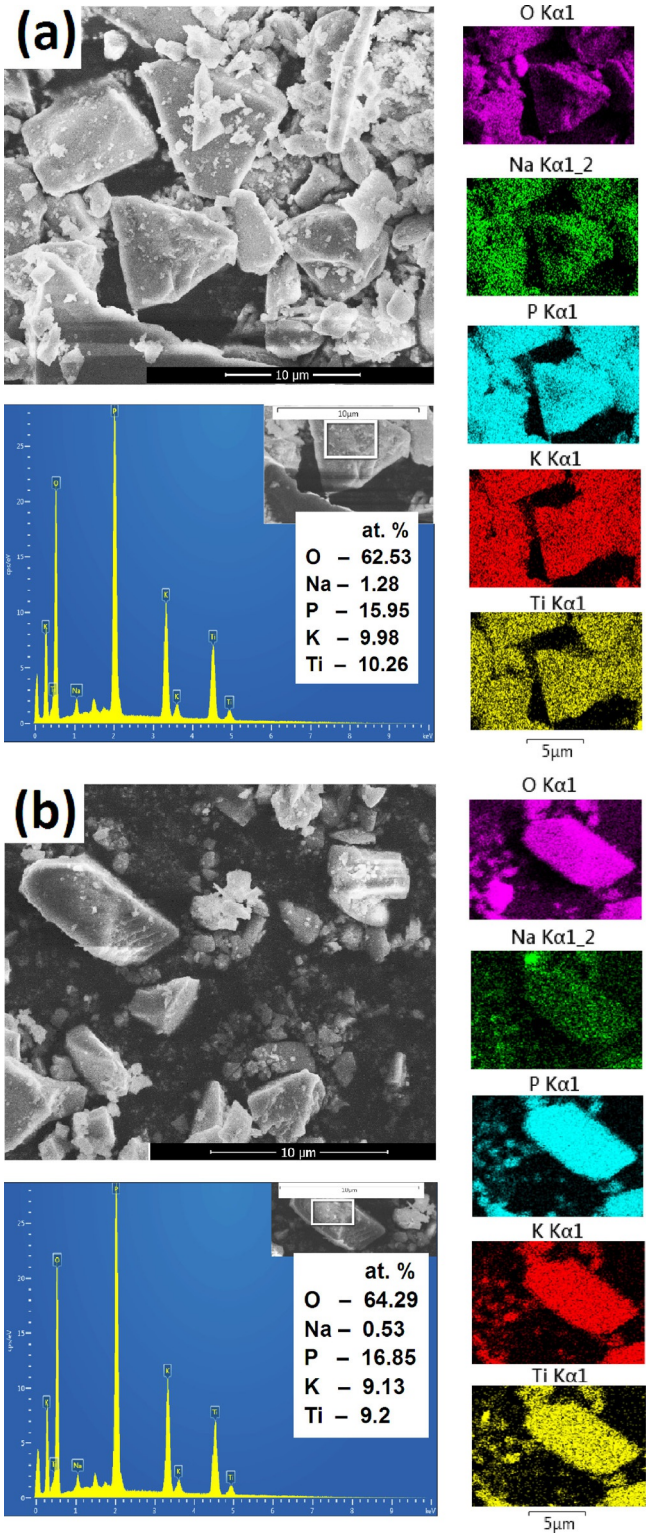

Figure 5. SEM images, EDS analysis, and mapping of the elements for separate crystals with different morphologies: a) $K_{2-x}Na_xTi_2(PO_4)_3$ ($x = 0.22–0.26$) solid solutions and b) $KTiP_2O_7$.

Heat treatment of the obtained mixture of phosphates was performed in air at 1173 K for 1 h to identify the sequence of

the thermal decomposition processes. This resulted in only a slight change in the violet shade of the sample. According to XRD, the crystalline phase of L-KNTP is preserved following heat treatment (Figure 1, curve 2), and the $KTiP_2O_7$ phosphate disintegrates almost completely and is present only as an impurity (less than 5 wt%). This indicates that air oxidation of trivalent titanium in $KTiP_2O_7$ at temperatures ranging from 823 to 1073 K leads to degradation of this compound with the formation of an amorphous product. At the same time, trivalent titanium in L-KNTP phosphate remains stable up to a temperature of 1300 K.

2.3. Crystal Structure of $K_{1.75}Na_{0.25}Ti_2(PO_4)_3$

For the X-ray diffraction study, a violet crystal of L-KNTP was selected. Refinement of the structure allowed determination of the composition of the investigated crystal. It is a solid solution of $K_{1.75}Na_{0.25}Ti_2(PO_4)_3$. The complex phosphate $K_{1.75}Na_{0.25}Ti_2(PO_4)_3$ is isostructural to the mineral langbeinite.[13] Selected bond lengths in the coordination polyhedra for this compound are listed in Table 1. The 3D framework contains isolated [TiO_6] octahedra and [PO_4] tetrahedra, which share vertices (Figure 6a).

Table 1. Bond lengths in the coordination polyhedra for $K_{1.75}Na_{0.25}Ti_2(PO_4)_3$.[a]

Polyhedra	Bond	Length [Å]	Bond	Length [Å]
TiO_6 polyhedra	Ti1–O4^{iv}	2.004(3)×3	Ti1–O3	2.020(3)×3
	Ti2–O1	1.918(2)×3	Ti2–O2^{xii}	1.952(3)×3
PO_4 tetrahedra	P3–O4	1.518(3)	P3–O3	1.520(3)
	P3–O2	1.539(3)	P3–O1	1.541(2)
K/NaO_x polyhedra	K/Na1–O1	2.893(3)×3	K/Na1–O4^{viii}	2.903(3)×3
	K/Na1–O2	2.932(3)×3	K/Na1–O2^{viii}	3.347(3)×3
	K2–O3^{vi}	2.807(3)×3	K2–O4^{iv}	2.926(3)×3
	K2–O2^{iv}	3.180(3)×3		

[a] Symmetry transformations used to generate equivalent atoms: iii) $x, -1+y, z$; iv) $0.5+y, 0.5-z, -x$; vi) $-x, 0.5+y, 0.5-z$; vii) y, z, x; viii) z, x, y; xii) $0.5+y, -0.5-z, -x$.

The two nearest [Ti(1)O_6] and [Ti(2)O_6] octahedra are linked by three orthophosphate bridges to form the [Ti(1)O_6(PO_4)$_3$Ti(2)O_6] building unit. The building blocks are assembled in three mutually orthogonal directions. Eight such blocks form a cavity with two types of sites, which are occupied by K(Na) cations.

The [Ti(1)O_6] and [Ti(2)O_6] octahedra are both slightly distorted (the titanium atoms appear displaced from the polyhedron center), and the corresponding Ti–O bond lengths are in the 1.918(2)–2.020(3) Å range (Table 1). The phosphorus atoms are tetrahedrally coordinated with P–O bond lengths in the range of 1.518(3) to 1.541(2) Å, which is normal for orthophosphate groups (Table 1).

There are two sites for alkaline metal atoms in the structure of $K_{1.75}Na_{0.25}Ti_2(PO_4)_3$ (Figure 6b). The first one, K/Na(1), is filled by sodium and potassium atoms in a ratio of 0.75:0.25. This site is surrounded by 9 oxygen atoms [assuming a cut-off value for the contact lengths of 2.932(3) Å] or by 12 oxygen atoms for contact lengths of 3.347(3) Å [the next-nearest contact is at 3.477(3) Å] (see Table 1). The potassium atom in the K(2) site forms nine K–O contacts in the 2.807(3)–3.180(3) Å range [the next distance, K(2)–O, is at 3.582(3) Å].

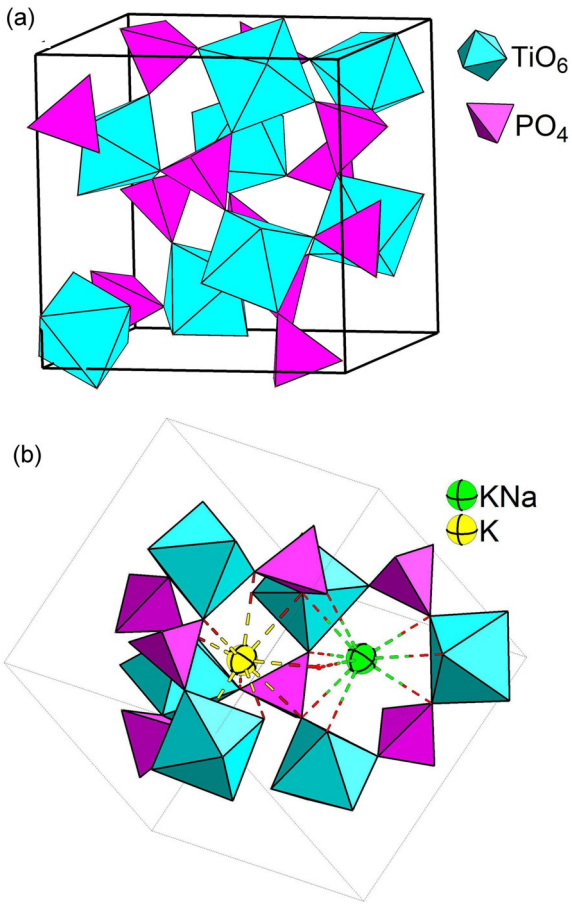

Figure 6. a) Linking of [TiO_6] octahedra and [PO_4] tetrahedra in the 3D framework of $K_{1.75}Na_{0.25}Ti_2(PO_4)_3$; b) oxygen environment of the K and K/Na atoms in a large cavity in the structure of $K_{1.75}Na_{0.25}Ti_2(PO_4)_3$.

The langbeinite-type $K_{0.877}Na_{0.48}Ti_2(PO_4)_3$ solid solution was obtained earlier,[27] for which the degree of substitution of potassium by sodium was greater than that in $K_{1.75}Na_{0.25}Ti_2(PO_4)_3$. We compared the results of the structural studies for these two compounds. In both cases, the construction principle of the anionic [$Ti_2(PO_4)_3$] sublattice is analogous. At the same time, for $K_{0.877}Na_{0.48}Ti_2(PO_4)_3$, less than 1/5 of the titanium atoms belong to the Ti^{III} positions, which causes a decrease in the Ti–O distances in the TiO_6 octahedra to 1.9052(19)–1.9719(17) Å. Accordingly, the charge of the anionic [$Ti_2(PO_4)_3$] sublattice for $K_{0.877}Na_{0.48}Ti_2(PO_4)_3$ is −1.357 e, which is less than that for $K_{1.75}Na_{0.25}Ti_2(PO_4)_3$. This causes the formation of vacant sites of the alkali metals in the structure. Thus, the crystallographic site of K/Na(1) in $K_{0.877}Na_{0.48}Ti_2(PO_4)_3$ is completely filled with equal portions of potassium and sodium atoms (K/Na = 0.52:0.48), and the K2 site is filled by potassium for only about a third of the amount (K_{vac}/K = 0.643:0.357). Notably, the formation of vacancies in only one of the alkali metal positions was observed earlier, for example, in a number of $Cs_{1+x}Ln_xZr_{2-x}(PO_4)_3$ (Ln = Sm–Lu) solid solutions.[22] The presence of vacancies significantly affects the geometry of the cavi-

ties in the anionic $[Ti_2(PO_4)_3]$ sublattice. In $K_{0.877}Na_{0.48}Ti_2(PO_4)_3$, the cavity for K/Na(1) [K/Na(1)–O bonds are in the 2.910(17)–3.044(2) Å range] is larger than that for K(2) [K(2)–O bonds range from 2.849(2) to 2.971(3) Å]. In contrast, the cavity for K/Na(1) sites in $K_{1.75}Na_{0.25}Ti_2(PO_4)_3$ is smaller than that for K(2) (see Table 1). So, the presence of vacant sites in the structure affects the possible degree of replacement of potassium by sodium.

To check the possible distribution of different elements over the same crystallographic positions and to compare the stability of obtained $K_{1.75}Na_{0.25}Ti_2(PO_4)_3$ relative to that of $K_2Ti_2(PO_4)_3$, the bond-valence sums (BVSs) were calculated by using a basic equation and parameters [Eq. (1)]:[29,30]

$$S = \exp[\frac{(R_0 - R)}{B}] \quad (1)$$

in which S is the bond valence, R is the bond length, R_0 is the empirically determined parameter,[29,30] and $B = 0.37$.[30] To compare the environments of the alkali metal sites, we modified the equation by the value of R_{0av} (average) [Eq. (2)]:

$$R_{0av} = R_0(K) \times R_{Oc}(K) + R_0(Na) \times R_{Oc}(Na) \quad (2)$$

in which R_{Oc} indicates partial occupancy of the site [$R_{Oc}(K) + R_0(Na) = 1$].

This approach was successfully applied for sites concurrently occupied by different elements in langbeinite-type frameworks in previous investigations.[22,31] As both $K_{1.75}Na_{0.25}Ti_2(PO_4)_3$ and $K_2Ti_2(PO_4)_3$ should contain equal quantities of Ti^{III} and Ti^{IV} due to their electroneutrality, three variants of BVS calculations for the positions of Ti1 and Ti2 were performed. They are as follows:

1) Ti^{III} is located in the Ti1 position, whereas Ti^{IV} is located in the Ti2 position;

2) Ti^{IV} is located in the Ti1 position, whereas Ti^{III} is located in the Ti2 position;

3) Ti^{III} and Ti^{IV} are distributed equiprobably over both the Ti1 and Ti2 positions with respective occupancies of 0.5 and 0.5; in this case, Equation (2) results in Equation (3):

$$R_0 = 0.5 \times R_0(Ti^{III}) + 0.5 \times R_0(Ti^{IV}) \quad (3)$$

the values of R_0(K), R_0(Na) $R_0(Ti^{III})$, and $R_0(Ti^{IV})$ were taken from Refs. [29, 30]. The results of the calculations are summarized in Table 2.

The reported values of the BVSs for alkaline metal sites are close to 1. The BVS value of the K1 position without taking into account the presence of Na gives a much higher value of 1.21, which confirms the correctness of the calculations with Equation (2) and localization of Na in the K1/Na1 position only. The difference in the BVS values of the Ti positions differs significantly for both sites (up to 1 for localization of Ti^{III} in the Ti1 position). For localization of Ti^{III} in the Ti2 position (variant 2), the BVS for Ti2 is lower (down to 4). In this case, taking into account that we operate with Ti^{III}, the value of the BVS is very high. So, we cannot assume that Ti^{III} is preferably located in the Ti2 position. At the same time, for the variant in which Ti^{III} is localized only in the Ti1 position, the common values of the BVSs for the Ti1 and Ti2 positions are also high. Only for equiprobable occupancy of Ti^{III} and Ti^{IV} over the Ti1 and Ti2 positions is the value of the BVS of Ti1 slightly lower than the theoretical value of 3.5, whereas the BVS of Ti2 is much higher than 3.5. Taking into account the calculated values, we can conclude that Ti^{III} is spread over both the Ti1 and Ti2 positions with possibly slightly higher occupancy in the Ti1 site. The BVS of P is close to 5. A slightly higher value of the total BVS for the formula unit depends on the obtained higher values of the BVS of Ti, which depends on the crystal structure and was reported in previous work.[31]

Table 2. Bond-valence sums for $K_{1.75}Na_{0.25}Ti_2(PO_4)_3$ and $K_2Ti_2(PO_4)_3$.

	Bond-valence sum $K_{1.75}Na_{0.25}Ti_2(PO_4)_3$			$K_2Ti_2(PO_4)_3$		
Variant	1	2	3	1	2	3
K/Na1		0.97[a]			0.97	
K2		1.01			1.06	
Ti1	3.30	3.52	3.41	3.32	3.54	3.43
Ti2	4.34	4.07	4.21	4.25	3.98	4.12
P1		4.97			5.05	
BVS for formula unit	24.53	24.48	24.51	24.75	24.7	24.73

[a] Calculated by using Equation (2).

Notably, only one of the crystallographic potassium sites in the L-KNTP structure is partially substituted by sodium. Preferable occupation of the K(1) position in L-KNTP by Na cations is substantiated by electronic structure calculations [a particular paper on the electronic structures of $K_{2-x}Na_xTi_2(PO_4)_3$ phosphates is in preparation]; however, in the Supporting Information we present some important results, namely, the calculated partial densities of states for $K_2Ti_2(PO_4)_3$ and $K_{1.75}Na_{0.25}Ti_2(PO_4)_3$ crystals [see Figures S5 and S6; for the optimized internuclear distances in $K_{1.75}Na_{0.25}Ti_2(PO_4)_3$, see Table S2]. The calculated energies of formation (E_f) for Na_K substitution in the K(1) and K(2) positions in $K_2Ti_2(PO_4)_3$ are −1.427 and −1.017 eV, respectively. The 0.41 eV difference definitely indicates that occupation of the K(1) position with Na is more energetically favorable. In general, negative E_f values for both the K(1) and K(2) positions for the Na_K defects substantiate thermodynamic stability of the synthesized $K_{1.75}Na_{0.25}Ti_2(PO_4)_3$ solid solution.

3. Conclusions

The features of the interactions of TiN with K_2O–Na_2O–P_2O_5 melts were investigated at different molar ratios [(Na + K)/P = 0.9, 1.0, and 1.2; Na/K = 1.0 and 2.0]. The obtained phosphates (K–Na-containing langbeinite-type complex phosphates and $KTiP_2O_7$) were investigated by using X-ray diffraction, scanning electron microscopy, FTIR spectroscopy, and thermogravimetric and differential thermal analysis methods. Langbeinite-type

$K_{1.75}Na_{0.25}Ti_2(PO_4)_3$ was characterized by single-crystal X-ray diffraction. According to structural analysis and calculation of the bond-valence sums, sodium atoms partially substitute potassium atoms only in one type of crystallographically inequivalent alkaline metal site. This factor may limit the degree of substitution of K by Na during the formation of $K_{2-x}Na_xTi_2(PO_4)_3$ solid solutions. Preferable occupation of the K(1) position was confirmed by DFT-based calculation of the formation energies of Na_K substitutional defects in the $K_2Ti_2(PO_4)_3$ lattice.

Experimental Section

Synthesis

All initial reagents, that is, $M^IH_2PO_4$, $M^I_2CO_3$ (M^I = Na, K), $NH_4H_2PO_4$, and TiN, were of analytical grade. The interaction of TiN with the molten Na_2O–K_2O–P_2O_5 system was investigated at (Na + K)/P molar ratios of 0.9, 1.0, and 1.2 and at Na/K molar ratios of 1.0 and 2.0 over the temperature range of 1173 to 1053 K. The Na_2O–K_2O–P_2O_5 starting systems were prepared by melting a homogeneous mixture at 1173 K: NaH_2PO_4 and KH_2PO_4 {(Na + K)/P = 1.0}; NaH_2PO_4, KH_2PO_4, and $NH_4H_2PO_4$ {(Na + K)/P = 0.9}; NaH_2PO_4, KH_2PO_4, Na_2CO_3, and K_2CO_3 {(Na + K)/P = 1.2}. Typical experimental procedures are described below. Finely powdered TiN (3.0 wt%) was added to the phosphate melts at 1173 K with stirring. The melts were exposed to this temperature for 1 h and were then cooled down to 1053 K at a rate of 40 K h^{-1}. At this temperature, fluxes containing crystals were poured from the crucible onto a copper sheet to freeze the crystallization processes. The crystalline phases were washed up from the residual melt with hot deionized water. All experiments were performed in air by using porcelain ware.

Characterization

The phase compositions of the obtained crystalline products were determined by powder X-ray diffraction (XRD) by using a Shimadzu XRD-6000 diffractometer (CuKα radiation, λ = 1.5418 Å; curved graphite monochromator on the counter arm; step size 0.02°; range 5–80°; scanning rate 2 s $step^{-1}$). Data collection for Rietveld refinement was performed in the 5–100° range (2θ step 0.02°) at a scanning rate of 8 s $step^{-1}$. The atomic coordinates of $K_{1.75}Na_{0.25}Ti_2(PO_4)_3$ (this investigation, CSD-432758) and $KTiP_2O_7$[32] were selected as starting models for Rietveld refinement. The observed, calculated, and difference X-ray patterns are shown in Figure 1.

The microstructure, morphology, chemical composition, and element mapping of the samples were analyzed by scanning electron microscopy (SEM, Magellan 400). EDS analysis (including element mapping) was performed for single crystals with different morphologies. Fourier-transform infrared spectroscopy (FTIR) was performed by using a PerkinElmer Spectrum BX spectrometer (in the 400–4000 cm^{-1} range; samples were pressed into discs with KBr). The weight loss and thermal behavior of the samples were investigated by using a Shimadzu DTG-60H simultaneous TG/DTA analyzer (heated in a platinum crucible under an air atmosphere at a rate of 10 K min^{-1} from room temperature to 1473 K; α-Al_2O_3 was used as a standard sample).

X-ray Experiments

X-ray experiments were performed with an Xcalibur Gemini diffractometer with a Ruby CCD detector (monochromated MoKα radiation, λ = 0.71073 Å) at 293 K. Crystal data and experimental conditions for intensity measurements and refinements are shown in Table 3. The structure was refined by using reference structure coordinates for an isotypic compound [$K_2Ti_2(PO_4)_3$, CSD-408970]. Initial atomic positions, isotropic displacement, and anisotropic displacement parameters were refined stepwise in order of decreasing X-ray scattering factors. Finally, sodium atoms were introduced to the model by populating the K(1) and K(2) positions equally and were refined by constraining the sum of the occupations. The positional disorder of Na(1)/K(1) ≈ 1/3 only survived during refinements, in contrast to unphysical occupancies at the K(2) site. Final atomic coordinates and site occupancies can be found in Table 4. Further details of the crystal structure investigation can be obtained from FIZ Karlsruhe, 76344 Eggenstein-Leopoldshafen, Germany (fax:

Table 3. Crystallographic data and structure refinement parameters for $K_{1.75}Na_{0.25}Ti_2(PO_4)_3$.

Formula	$K_{1.75}Na_{0.25}Ti_2(PO_4)_3$
Crystal system	cubic
Space group	$P2_13$
Cell parameter [Å], a	9.851(5)
V [Å^3]	956.0(15)
Z	4
ρ_{calcd} [g cm^{-3}]	3.160
Crystal dimensions [mm]	0.1097 × 0.0948 × 0.0830
Apparatus	Xcalibur Gemini
λ [Å]	0.71073
Monochromator	graphite
μ [mm^{-1}]	3.005
Absorption correction	multi-scan
T_{min}, T_{max} [°C]	0.794, 0.813
No. reflns	5433
Independent reflns	924
Reflns with $>2\sigma(I)$	898
θ_{min}, θ_{max} [°]	3.582; 29.990
h, k, l	−13→13, −12→9, −12→13
R_1(all)	0.0209
wR_2	0.0526
S_{all}	1.135
No. parameters	59
Flack parameter	0.011(17)
$\Delta\rho_{max}$, $\Delta\rho_{min}$ [e Å^{-3}]	0.369, −0.347

Table 4. Atomic coordinates, their equivalent anisotropic parameters, and sites occupation for $K_{1.75}Na_{0.25}Ti_2(PO_4)_3$.

Atom	Site	Occupancy	x/a	y/b	z/c	U_{eq} [Å^2]
Ti1	4a	1	0.1075(1)	0.1075(1)	0.1075(1)	0.0068(2)
Ti2	4a	1	0.3375(1)	−0.3375(1)	0.1625(1)	0.0059(2)
P3	12b	1	0.0245(1)	−0.2093(1)	0.1221(1)	0.00558(16)
K1	4a	0.75	0.1844(1)	−0.3156(1)	−0.1844(1)	0.0182(6)
Na1	4a	0.25	0.1844(1)	−0.3156(1)	−0.1844(1)	0.0182(6)
K2	4a	1	−0.0441(1)	0.4559(1)	0.0441(1)	0.0222(3)
O1	12b	1	0.1740(2)	−0.2508(2)	0.1019(3)	0.0117(5)
O2	12b	1	−0.0450(3)	−0.2271(3)	−0.0166(2)	0.0138(5)
O3	12b	1	0.0160(3)	−0.0639(2)	0.1730(3)	0.0117(5)
O4	2b	1	−0.0485(3)	−0.3041(3)	0.2191(3)	0.0142(5)

+49 7247-808-666; e-mail: crysdata@fiz-karlsruhe.de) on quoting the depository numbers CSD-432758.

Calculation Method

The electronic structure calculations presented in this paper were aimed to determine the most energetically favorable positions for Na_K substitutional defects in the $K_2Ti_2(PO_4)_3$ host. This task was solved by comparing the defect formation energies calculated for different cases of Na occupation. According to the structural data, a regular unit cell of $K_2Ti_2(PO_4)_3$ contains two inequivalent sites for Na_K substitution, K(1) and K(2).[15] The formation energy (E_f) of the Na_K defect in the $K_2Ti_2(PO_4)_3$ host was evaluated by using a generally accepted equation [Eq. (4)]:

$$E_f = E_{total}[K_2Ti_2(PO_4)_3/Na] - E_{total}[K_2Ti_2(PO_4)_3] - [E_{total}(Na) - E_{total}(K)] \quad (4)$$

in which the first two terms are the total energies of defective and perfect $K_2Ti_2(PO_4)_3$ crystals and $E_{total}(Na)$ and $E_{total}(K)$ the are total energies of sodium and potassium metal calculated per atom. A negative value of E_f indicates thermodynamic stability of the target compound.

The unit cell of the $K_2Ti_2(PO_4)_3$ crystal (cubic system lattice with the $P2_13$ symmetry group #198) contains four formula units of $K_2Ti_2(PO_4)_3$ and correspondingly eight K atoms. To model the Na-doped crystal, the unit-cell symmetry of $K_2Ti_2(PO_4)_3$ was set to the trivial group $P1$, thus providing eight inequivalent K atoms, four of which were on K(1) and the remaining four of which were on the K(2) positions. Then, one K atom [either in the K(1) or K(2) position] was replaced by Na to provide the $K_{1.75}Na_{0.25}Ti_2(PO_4)_3$ chemical formula of the Na-containing crystal. The total energy of a perfect $K_2Ti_2(PO_4)_3$ crystal was also calculated by setting the unit-cell symmetry as $P1$.

The electronic structure calculations were performed in spin-polarized mode by using the DFT-based plane-wave pseudopotential method implemented in the CASTEP package[33] distributed inside a computational commercial pack.[34] The ion–electron interactions were modeled by Vanderbilt-type nonlocal ultrasoft pseudopotentials.[35] The following orbital electrons were regarded as valence electrons: O $2s^22p^4$, Na $2s^22p^63s^1$, P $3s^23p^3$, K $3s^23p^64s^1$, Ti $3s^23p^63d^24s^2$. Perdew–Burke–Ernzerhof (PBE) was used to calculate the exchange-correlation effects in the generalized gradient approximation (GGA).[36] The energy cutoff of plane-wave basis set was 340.0 eV with Monkhorst–Pack k-point mesh with a separation of 0.07 $Å^{-1}$ in the Brillouin Zone. No initial spin states of atoms were assigned. Additional convergence tests showed that the choice of above computational parameters was sufficiently accurate in this study.

Geometry optimizations were performed only for atomic positions in the $P1$-symmetry unit cells of $K_{1.75}Na_{0.25}Ti_2(PO_4)_3$ and $K_2Ti_2(PO_4)_3$ crystals with constrained unit-cell parameters. The unit-cell parameters and initial atomic coordinates were taken from the literature (CSD-408970).[15] The optimization was performed by the Broyden–Fletcher–Goldfarb–Shanno (BFGS) minimization technique[37] by using the following convergence criteria: energy tolerance of 10^{-5} eVatom^{-1}, maximum Hellman–Feynman forces 0.03 eV $Å^{-1}$, and maximum stress and maximum displacement 0.05 GPa and 10^{-3} Å, respectively.

The $E_{total}(Na)$ and $E_{total}(K)$ energies of sodium and potassium metal were calculated by using the same parameters and approximations as for the phosphate crystals (sodium and potassium metal possess body-centered cubic lattice with symmetry group #229 and lattice constants $a = 4.2906$ and 5.3280 Å, respectively).

Acknowledgements

This work was supported by the national long-term project [no. WQ20142200205] of "Thousand Talents Plan of Bureau of Foreign Experts Affairs" of People's Republic of China. Electronic structure calculations were done with the use of supercomputer equipment of Shenzhen Cloud Computing Center, National Supercomputing Center in Shenzhen, People's Republic of China. The authors deeply acknowledge Prof. Dr. Santiago Garcia-Granda, Mr. Rafael Mendoza Meroño (Department of Physical and Analytical Chemistry, University of Oviedo, Spain), and Ph.D. Artem Babaryk (Taras Shevchenko National University, Kyiv, Ukraine) for single-crystal X-ray data collection and discussion of the results. We are also grateful to Prof. Li Yi and Mr. Li Lin (State Key Laboratory of Inorganic Synthesis and Preparative Chemistry, Jilin University) for help with the calculations.

Conflict of Interest

The authors declare no conflict of interest.

Keywords: crystal structure · electron microscopy · potassium · sodium · X-ray diffraction

[1] H.-K. Song, K. Lee, M. Kim, L. Nazar, J. Cho, *Adv. Funct. Mater.* **2010**, *20*, 3818 – 3834.
[2] C. Masquelier, L. Croguennec, *Chem. Rev.* **2013**, *113*, 6552 – 6591.
[3] D. Kundu, E. Talaie, V. Duffort, L. Nazar, *Angew. Chem. Int. Ed.* **2015**, *54*, 3431 – 3448; *Angew. Chem.* **2015**, *127*, 3495 – 3513.
[4] K. Lee, T. Ramesh, F. Nan, G. Botton, L. Nazar, *Chem. Mater.* **2011**, *23*, 3593 – 3600.
[5] V. Palomares, M. Casas-Cabanas, E. Castillo-Martınez, M. Hanb, T. Rojo, *Energy Environ. Sci.* **2013**, *6*, 2312 – 2337.
[6] B. Senthilkumar, K. Sankar, L. Vasylechko, Y.-S. Lee, R. Selvan, *RSC Adv.* **2014**, *4*, 53192 – 53200.
[7] B. Ellis, W. Makahnouk, W. Rowan-Weetaluktuk, D. Ryan, L. Nazar, *Chem. Mater.* **2010**, *22*, 1059 – 1070.
[8] B. Senthilkumar, G. Ananya, P. Ashok, S. Ramaprabhu, *Electrochim. Acta* **2015**, *169*, 447 – 455.
[9] M. Nose, K. Nobuhara, S. Shiotani, H. Nakayama, S. Nakanishia, H. Iba, *RSC Adv.* **2014**, *4*, 9044 – 9047.
[10] L. Lander, G. Rousse, D. Batuk, C. V. Colin, D. Alves Dalla Corte, J.-M. Tarascon, *Inorg. Chem.* **2017**, *56*, 2013 – 2021.
[11] S. Abrahams, J. Bernstein, *J. Chem. Phys.* **1966**, *45*, 2745 – 2752.
[12] C. Burba, R. Frech, *Solid State Ionics* **2007**, *177*, 3445 – 3454.
[13] A. Zemann, J. Zemann, *Acta Crystallogr.* **1957**, *10*, 409 – 413.
[14] A. Leclaire, A. Benmousa, M. Borell, A. Grandin, B. Raveau, *J. Solid State Chem.* **1989**, *78*, 227 – 231.
[15] I. V. Zatovsky, N. S. Slobodynik, D. A. Stratiychuk, K. V. Domasevitch, J. Sieler, E. B. Rusanov, *Z. Naturforsch. B* **2000**, *55*, 291 – 298.
[16] D. Zhao, H. Zhang, S.-P. Huang, W.-L. Zhang, S.-L. Yang, W.-D. Cheng, *J. Alloys Compd.* **2009**, *477*, 795 – 799.
[17] S. Norberg, *Acta Crystallogr. Sect. B.* **2002**, *58*, 743 – 749.
[18] I. Ogorodnyk, I. Zatovsky, N. Slobodyanik, *Russ. J. Inorg. Chem.* **2007**, *52*, 121 – 126.

[19] I. Ogorodnyk, I. Zatovsky, N. Slobodyanik, V. Baumer, O. Shishkin, *J. Solid State Chem.* **2006**, *179*, 3461 – 3466.
[20] J. Gustafsson, S. Norberg, G. Svensson, J. Albertsson, *Acta Crystallogr. Sect. C* **2005**, *61*, i9 – i13.
[21] J. Liu, X. Duan, Y. Zhang, Z. Li, F. Yu, H. Jiang, *J. Alloys Compd.* **2016**, *660*, 356 – 360.
[22] I. Ogorodnyk, V. Baumer, I. Zatovsky, N. Slobodyanik, O. Shishkin, K. Domasevitch, *Acta Crystallogr. Sect. B* **2007**, *63*, 819 – 827.
[23] A. Orlova, K. Koryttseva, E. Loginova, *Radiochemistry* **2011**, *53*, 51 – 62.
[24] L. Niu, W. Liang, Z. Wu, Y. Wang, *Adv. Mater. Res.* **2014**, *936*, 585 – 590.
[25] J. Isasi, A. Daidouh, *Solid State Ionics* **2000**, *133*, 303 – 313.
[26] K. Rangan, J. Gopalakrishnan, *J. Solid State Chem.* **1994**, *109*, 116 – 121.
[27] N. Strutynska, M. Bondarenko, N. Slobodyanik, V. Baumer, I. Zatovsky, K. Bychkov, A. Puzan, *Cryst. Res. Technol.* **2016**, *51*, 627 – 633.
[28] V. Kurazhkovskaya, A. Orlova, V. Petkov, D. Kemenov, L. Kaplunnik, *J. Struct. Chem.* **2000**, *41*, 61 – 66.
[29] I. Brown, D. Altermatt, *Acta Crystallogr. Sect. B* **1985**, *41*, 244 – 247.
[30] N. Brese, M. O'Keeffe, *Acta Crystallogr. Sect. B* **1991**, *47*, 192 – 197.
[31] N. Slobodyanik, K. Terebilenko, I. Ogorodnyk, I. Zatovsky, M. Seredyuk, V. Baumer, P. Gutlich, *Inorg. Chem.* **2012**, *51*, 1380 – 1385.
[32] I. Zatovsky, N. Slobodyanik, A. Kowalski, T. Slyva, *Dopov. Nats. Akad. Nauk Ukr.* **2000**, *3*, 151 – 155.
[33] M. Payne, M. Teter, D. Allan, T. Arias, J. Joannopoulos, *Rev. Mod. Phys.* **1992**, *64*, 1045 – 1097.
[34] Materials Studio, version 8.0, Accelrys Inc., San Diego, **2007**.
[35] R. Kari-Laasonen, C. Lee, D. Vanderbilt, *Phys. Rev. B* **1991**, *43*, 6796 – 6799.
[36] J. Perdew, K. Bunrke, M. Ernzerhof, *Phys. Rev. Lett.* **1996**, *77*, 3865 – 3868.
[37] B. Pfrommer, M. Cote, S. Louie, M. Cohen, *J. Comput. Phys.* **1997**, *131*, 233 – 240.

Received: April 16, 2018
Version of record online June 20, 2018

